ELSEVIER

Thermochimica Acta 280/281 (1996) 319–332

thermochimica acta

Nucleation and coalescence phenomena in the transformation of semiconductor-doped glasses[1]

Subhash H. Risbud

Division of Materials Science and Engineering, Department of Chemical Engineering and Materials Science, University of California, Davis, CA 95616, USA

Abstract

The nucleation, coalescence and growth of semiconductor particles precipitated from supersaturated silicate and phosphate glasses have been investigated using a number of II-IV, III-V and elemental semiconductor particles. The nucleation phenomena and the resulting microstructure are of intense interest for optical device applications and have become one useful way of creating quantum dot structures. This overview highlights the processing, structure, and thermodynamic-kinetic aspects of these nanophase composite materials with a special focus on the optical absorption, luminescence of the glasses after the "striking" heat treatments.

Keywords: Glass; Microstructure; Nucleation; Semiconductor

1. Introduction

The preparation, processing, and optical property studies of semiconductor quantum dots is an exciting area of research because of the high likelihood that such materials will impact many new technologies including flat panel displays, light emitting materials, and nanoelectronics. For example, the development of light emitting diodes (LED) and semiconductor lasers is critically dependent on materials capable of efficient light emission in the visible and UV regime. Ever since the discovery of the transistor [1] electronic devices have continued a trend toward smaller and smaller sizes with the attendant challenges of nanosize materials processing. The processing science of semiconductors of a size small enough (nanometers) to achieve quantum confinement effects, preferably in all three spatial dimensions (quantum dots),

[1] Dedicated to Professor Hiroshi Suga.

SSDI 0040-6031(95)02650-9

has made rapid progress in the last 10 years and represents perhaps the best integration of materials synthesis, quantum physics, and state-of-the-art electronic and photonic technologies. The device applications of quantum wells, superlattices, and quantum wires and dots [2] have spurred a revolution in the speed of signal processing and miniaturization of circuitry.

The purpose of the present paper is to give a background on quantum dot particles from the perspective of the fundamental concepts, synthesis methods, and the nucleation and growth transformations that are important in the preparation of these materials.

2. Background and literature

In theory, a conduction electron or hold confined three-dimensionally in a nanometer-size semiconductor microcrystallite behaves more like a de Broglie wave than like a classical particle. Some discrete energy levels exist between the conduction and valence bands in such a nanosize semiconductor with size-dependent energy gaps. To examine these theoretically predicted properties of quantum dots and develop possible applications, many technologies have been used to fabricate quantum dots in different types of systems (see Table 1). Quantum dots have been formed as colloidal suspension in liquid solutions [3–6] or polymer films [7], by precipitation (striking) processes in glasses [8–12] or crystals [13], by chemically synthesized colloidal-entrapment in zeolites [14] or Vycor glasses [15], by colloidal suspension with sol-gel processing[16], by molecular-beam epitaxy (MBE) with electron-beam lithography [17, 18], and by magnetron sputtering of thin films [19].

Table 1
Quantum-dot Fabrication methods

Method	Quantum structure	Medium
Colloidal suspension	ZnS, ZnSe, CdS	Liquid
Organometallic synthesis	GaAs, CdS	Powder
Collodial suspension	CdS	Nafion
Collodial entrapment	CdS, PbS	Zeolite
Collodial entrapment	GaAs	Vycor
Collodial suspension	CdS	Silica glasses (sol-gel)
Glass precipitation	CdS, CuCl, CuBr	Silicate glasses (melting)
Glass precipitation	CdS, CdSe, CuCl, AgI	Silicate glasses (melting)
Glass precipitation	CdS, CdSe, CdTe	Silicate glasses (melting)
Crystal precipitation	CuCl	NaCl
Molecular beam epitaxy and electron beam lithography	InGaAS–AlGaAs–GaAs	–
Magnetron sputtering	CdTe, CdSe, GaAs	Silica glass thin film
Hydrofloride etching	porous silicon (quantum wires)	–
Glass dissolution and suspension	Si, GaAs	Silicate glasses (melting)

In our laboratory, we form quantum dots by the process of precipitation in silicate glasses originally developed to make color filter glasses. Glass melting, fast quenching, and careful heat treatment are the three major materials preparation steps and they involve dissolving the semiconductor in the glass melt during high-temperature melting, forming supersaturated solutions during fast quenching, then nucleating, growing, and coarsening quantum dots in glass by heat treatment. The formation of nanometer size quantum dots through these heat treatments constitute the major advantage of this fabrication technique, while the low solubility of semiconductors in silicate glasses and the broad quantum-dot size distribution [10, 11, 20] are among the disadvantages.

The major features of the quantum confinement effects of quantum dots are the size-dependent shift of the optical absorption edge, some excitonic absorption peaks on the shoulder of the absorption edge at room temperature [3, 8, 10, 12], and the electric-field-modulated optical absorption (quantum-confined Franz–Keldysh effect) [21, 22]. The large third-order optical nonlinearity and ultra-fast response time of these room-temperature excitonic peaks with or without electric field modulation is attractive for femto-second photonic switching and electro-optical modulation devices in photonic technologies. Semiconductor quantum-dot lasers are expected to have superior characteristics, such as extremely low threshold currents, less temperature dependence and narrow grain spectra, compared to conventional double-heterostructure lasers. Moreover, high-quality quantum dots in glasses can be used as nonlinear optical-waveguide materials due to the well-established optical fiber processing industry. Quite recently, various HF-etched porous-silicon nanostructures have been shown to emit luminescence upon photo and electric excitation [23,24]. These optical phenomena have attracted wide attention and research interest due to the possible connection of the light emission to quantum confinement effects of the nanosize silicon quantum wires and quantum dots [25].

The coloration caused by microcrystallite precipitation in glasses is vividly seen in some of the commercial cut-off filter glasses made by Corning and Schott Glass Companies. These glasses exhibit two or three absorption peaks other than the simple absorption edge shifts corresponding to different stages of heat treatment. Combining the microstructural data and the absorption spectra, the absorption edge shifts can be attributed to the size-dependent energy gap of semiconductor microcrystallites. The absorption peaks on the shoulder of the absorption edge can be explained as quantum-confined exciton-transition peaks. The easy availability of these commercial cut-off color glasses led to early studies of quantum confinement effects but commerical glasses were not originally designed for the study of these new physical phenomena. In fact, it is impossible to avoid mixed microcrystallites in these materials and thus the best samples for research are carefully designed base-glass compositions with deliberate semiconductors additions.

3. Semiconductor quantum dots in glasses

The first convincing results in well-designed experimental glasses were reported by Ekimov and Onushchenko [8]. There, CdS microcrystallites of radii 1.4–38 nm

exhibited very pronounced absorption-edge shifts. The particles with average radius 1.9 nm showed three well-defined absorption peaks corresponding to the three different energy-level transitions of the CdS quantum dots. The overgrown CdS-particles (with average radius ~ 38 nm), in particular, exhibited a steep and smooth bulk-CdS absorption edge at room temperature and three sharp bulk-CdS exciton absorption peaks at 4.2 K. These findings strongly suggest that the particles grown from the glass matrices are indeed CdS microcrystallites, all the way from radii 1.4 to 38 nm. Ekimov and Onushchenko also used a small angle X-ray scattering (SAXS) technique for measuring the CdS- and CuCl-microcrystallite sizes, then proved that the size-growth rates of the precipitated CdS-and CuCl-particles under various heat-treatment temperatures and times follow the well-known Lifshitz–Slyozov–Wagner (LSW) coarsening-rate equation. Our recent work has provided a better theoretical model for coarsening kinetics based on in situ hot-stage high-voltage transmission electron microscopy studies [26].

The solubility of semiconductors in glasses is one critical factor for producing successful semiconductor quantum dots in the glass matrices. Generally speaking, the molten silicate glasses can dissolve only a small group of semiconductors (especially the II-VI family). Therefore, we must deal with the dissolution rates of the added semiconductors in the glass melts, especially for the truncated-dissolution nanocrystal remnants of certain types of semiconductor, such as Si and GaAs.

In any transformations involving long-range transport, the diffusion equation

$$D\left[\frac{\partial^2 C}{\partial x^2}+\frac{\partial^2 C}{\partial y^2}+\frac{\partial^2 C}{\partial z^2}\right]=D\nabla^2 C=\frac{\partial C}{\partial t'} \tag{1}$$

must be satisfied. Considering an isolated spherical semiconductor nanocrystal in an infinite glass melt, D is the diffusion coefficient [27] of the added semiconductor atoms in the glass melt and $C=C(r,t)$ is the concentration field (a function of time t and distance r to the center of the nanocrystal) of semiconductor atoms in the melt surrounding the nanocrystal, subject to the conditions

$$\begin{aligned} &C(r=R,t)=C_{\mathrm{i}}(0<t\leq\infty)\\ &\text{and}\quad C(r,t=0)=C_{\mathrm{m}}(r>R)\\ &\text{and}\quad C(r=\infty,t)=C_{\mathrm{m}}(0\leq t\leq\infty) \end{aligned} \tag{2}$$

where $r=R$ at the nanocrystal/glass melt interface, C_{i} is the concentration in the melt at the interface, and C_{m} is the glass melt composition at a point remote from the nanocrystal. The flux balance must also be satisfied

$$(C_{\mathrm{n}}-C_{\mathrm{i}})\frac{dR}{\mathrm{d}t}=D\left[\frac{\partial C}{\partial r}\right]_{r=R} \tag{3}$$

where C_{n}, the composition of the nanocrystal, is assumed constant and independent of r and t; and $R=R_{\mathrm{o}}$ at $t=0$.

The dissolution velocity of a spherical nanocrystal (with radius R) can be obtained from the flux balance equation

$$\frac{dR}{dt} = -k\left[\frac{D}{R} + \left(\frac{D}{\pi t}\right)^{1/2}\right] \tag{4}$$

where $k = 2(C_i - C_m)/(C_n - C_i)$ describes the supersaturation of semiconductor atoms in the glass melt.

The classical nucleation theory might describe the first stage of semiconductor quantum-dot precipitation from the supersaturated solid solution. Using the steady-state homogeneous nucleation as our first approximation, the nucleation rate is given by

$$I = A\exp\left[-\frac{\Delta G_c + \Delta G_a}{RT}\right] \tag{5}$$

where

$$\Delta G_c = \frac{16\pi\sigma^3}{3\Delta G_v^2} \tag{6}$$

is the critical excess free energy, ΔG_a is the activation energy associated with the jump of atoms across the nucleus/matrix interface, ΔG_v is the bulk free energy decrease per unit volume, σ is the interface free energy per unit area, R is the ideal gas constant, T is the temperature in degrees K, A is the proportionality constant, and the critical radius of the nuclei $r^* = 2\sigma/\Delta G_v$. Therefore, we can obtain

$$I = A\exp\left[-\frac{\Delta G_a}{RT}\right]\exp\left[-\frac{4\pi\sigma r^{*2}}{3RT}\right] \tag{7}$$

which describes approximately the nucleation rate of the first stage of quantum-dot precipitation in glass matrices. It is not likely that the nucleation processes in the glass matrices occur homogeneously. However, very uniformly distributed quantum dots in the glass matrices were usually observed through transmission electron microscopy. This differs considerably from the crystallization processes of the glass matrices, which usually occur on the surfaces or flaws of the glasses. It will be quite interesting to study the early-stage precipitation process more precisely to understand the nature of quantum-dot nucleation in the glass matrix.

At higher temperature for longer times, the nucleated quantum dots might experience normal growth. For normal growth in a strain-free matrix, the growth rate is given by

$$g = \frac{dr}{dt} = \alpha M\gamma r^{-1} \tag{8}$$

and the quantum-dot grain-boundary mobility by

$$M = \frac{A'}{T}\exp\left[-\frac{\Delta G_a'}{RT}\right] \tag{9}$$

Thus the normal growth equation can be expressed as

$$r^2 = r_0^2 + Kt \tag{10}$$

where A' is a proportionality constant, $\Delta G'_a$ is the normal growth activation energy, $K = \alpha M \gamma$ is the normal growth coefficient, α is another proportionality constant of the order of unity, γ is the quantum-dot boundary energy, r is the mean dot radius, and r_0 is the initial mean radius.

Neglecting the initial mean radius, we assume $r \approx t^{1/2}$ as a relationship for the quantum-dot mean radius versus their heat treatment time. In the experimental work of Fuyu et al. [28,29] on Cd(S, Se)-doped glasses, indirect evidence for an $r \approx t^{1/2}$ relationship during a possibly normal growth stage was obtained. These results were based on estimations of cluster size from the shift of the optical absorption edge with heat treatment time; the activation energy for normal growth was estimated to be ≈ 329 kJ mol^{-1}.

As the concentration of the semiconductor in the supersaturated glass solution approaches the solubility limit (or equilibrium concentration C_e), normal growth is taken over by a coarsening (or coalescence) process. During the coarsening stage of quantum dots, the particle radius distribution can be expressed as

$$P(u) = 3^4 2^{-5/3} e u^2 (u+3)^{-7/3} \left(\frac{3}{2} - u\right)^{-11/3} \exp\left[\left(\frac{2u}{3} - 1\right)^{-1}\right] \tag{11}$$

for $(u \leq 3/2)$ and $P(u) = 0, (u > 3/2)$, where $u = r/r^*$, r is the cluster radius, and r^* is the critical radius of clusters. The cluster coarsening equation is given by

$$r_{av} = r^* = \left[\frac{4\alpha D t}{9}\right]^{1/3} \tag{12}$$

where

$$\alpha = \frac{2\sigma v^2 C_e}{kT} \tag{13}$$

and

$$D = D_0 \exp\left[-\frac{\Delta G_{coar}}{RT}\right] \tag{14}$$

where v is the atomic volume, ΔG_{coar} is the activation energy of coarsening, k is the Boltzmann constant, and D is the diffusion coefficient.

The above equations can be used to obtain the following equations relating the quantum-dot average radius r_{av} to the heat treatment times t of the quantum dots in glasses

$$s^3 = \left[\frac{r_{av}}{t^{1/3}}\right]^3 = \left[\frac{B}{T}\right] \exp\left[-\frac{\Delta G_{coar}}{RT}\right] \tag{15}$$

i.e.

$$t = \left[\frac{r_{av}^3}{B}\right] T \exp\left[\frac{\Delta G_{coar}}{RT}\right] \tag{16}$$

where S is the slope of the r_{av}–$t^{1/3}$ straight line plot [30] and B is the proportionality constant. Eq. (15) has a practical significance for optimizing the heat treatments of quantum dots in glasses based on the time–temperature (t–T) plots as shown in Fig. 1.

We analyzed experimental data on CdS-doped glasses reported by Ekimov et al. [30]. We found that data on the average quantum-dot radius obey the $r_{av} \approx t^{1/3}$ relationship as expected from the above for the particle coarsening stage. Using the size–time–temperature data of Ekimov et al. we then constructed t–T plots (Fig. 1) for use in precipitating quantum dots of sizes comparable to the exciton Bohr radius ($\approx$ 3 nm for CdS). We used the t–T plots as master curves to guide heat treatments and yield CdS quantum-dot samples showing reproducible and pronounced quantum confinement effects. The activation energy for diffusion in the coarsening regime estimated from t–T curves is found to be $\approx$ 345 kJ mol^{-1} for CdS-doped glasses. These data compare reasonably with values of 329 kJ mol^{-1} for normal growth and 313 kJ mol^{-1} for the coarsening regime, as reported by Fuyu et al. [28, 29] for Cd(S, Se)-doped glasses. All of these estimated activation energy values are quite close to the heats of formation of CdS (402 kJ mol^{-1}) and CdSe (377 kJ mol^{-1}).

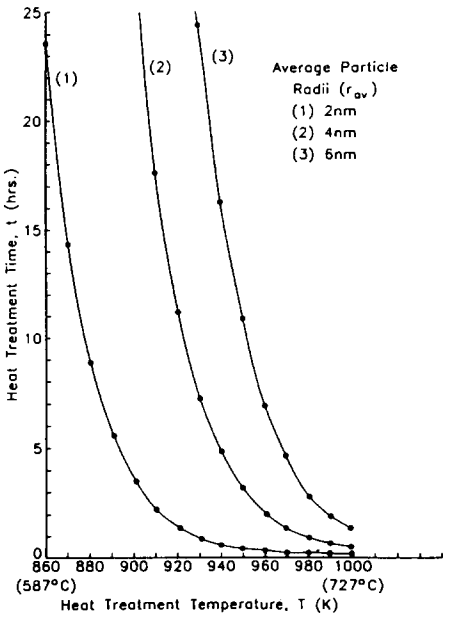

Fig. 1. Theoretical time–temperature curves for precipitating CdS quantum dots with 2 nm, 4 nm, and 6 nm average radii.

While the results above show that normal growth and LSW coarsening theories apply to the quantum dots in glasses reasonably well, the growth equations (10) and (12) all show an infinite radius versus infinite time feature, which seems unrealistic for the growth of quantum dots in glasses. We have recently analyzed and proposed a model for growth and coarsening of CdS in glasses [26].

4. Experimental methods and results

4.1. CdS and CdSe in silicate glasses

We have prepared over one hundred samples of CdS and CdSe quantum dots in silicate glasses by co-melting 1–3 wt% of the semiconductor with one of the experimentally developed silicate-glass compositions shown in Table 2. Since we could not obtain phase diagrams of compositions containing more than three oxides for the glass compositions, we found it necessary to use differential thermal analysis (DTA) for determining relatively stable base-glass compositions for doping semiconductors. Choosing stable base glasses avoided glass phase separation or glass crystallization during the striking process for precipitating quantum dots. In melting the glasses, excess CdS or CdSe was added to compensate for anticipated vaporizations losses, with the retained concentration of the semiconductor estimated to be not less than 10 or 15% of the batched amount. Fine glass semiconductor powders (25–30 g) were pre-mixed and melted in alumina crucibles at 1400 C for 1.5 h. The melts were rapidly quenched by pouring onto a brass plate to obtain clear glass sheets. Then DTA was performed to guide the choice of glass heat-treatment conditions. Sections from the as-quenched clear glass were subjected to striking in the temperature range 577–735°C for varying times to promote the nucleation and growth of nanocrystallites in the glass. Glasses in shades of light yellow, orange, ruby red to dark brown (for CdSe quantum dots) and light greenish-yellow to bright yellow (for CdS quantum dots) were polished to obtain uniform samples of 1-mm-thickness for optical spectroscopic analyses. Batch

Table 2
Composition of glasses compatible with II-VI quantum dots

Glass B-4		Glass B-9	
Component	Amount/wt%	Component	Amount/wt%
SiO_2	56	SiO_2	54.50
B_2O_3	8	B_2O_3	22.660
K_2O	24	K_2O	6.600
CaO	3	CaO	0.825
BaO	9	BaO	2.475
		Na_2O	2.26
		Al_2O_3	1.056
		ZnO	9.800

compositions, melting, and heat-treatment conditions were optimized by evaluating the sharpness and position of the quantum-confinement peaks in the linear absorption spectrum. Samples for transmission electron microscopy were prepared by successive mechanical polishing, dimpling, and ion milling.

Fig. 2 shows DTA traces of undoped base glass and CdS-doped glass, respectively. The CdS-doped glass has a glass transition temperature of ~ 577°C followed by a crystallization onset T_c of ~ 735 C; the base glass without CdS has a crystallization onset T_c of ~ 768 C. The crystallization exotherms seen in the DTA traces must correspond to bulk devitrification or crystal growth of oxide phase in the glass matrix since thermal effects of this magnitude are not expected due to the early-stage nucleation of CdS. The lower T_c observed in the CdS-doped glass sample suggests that

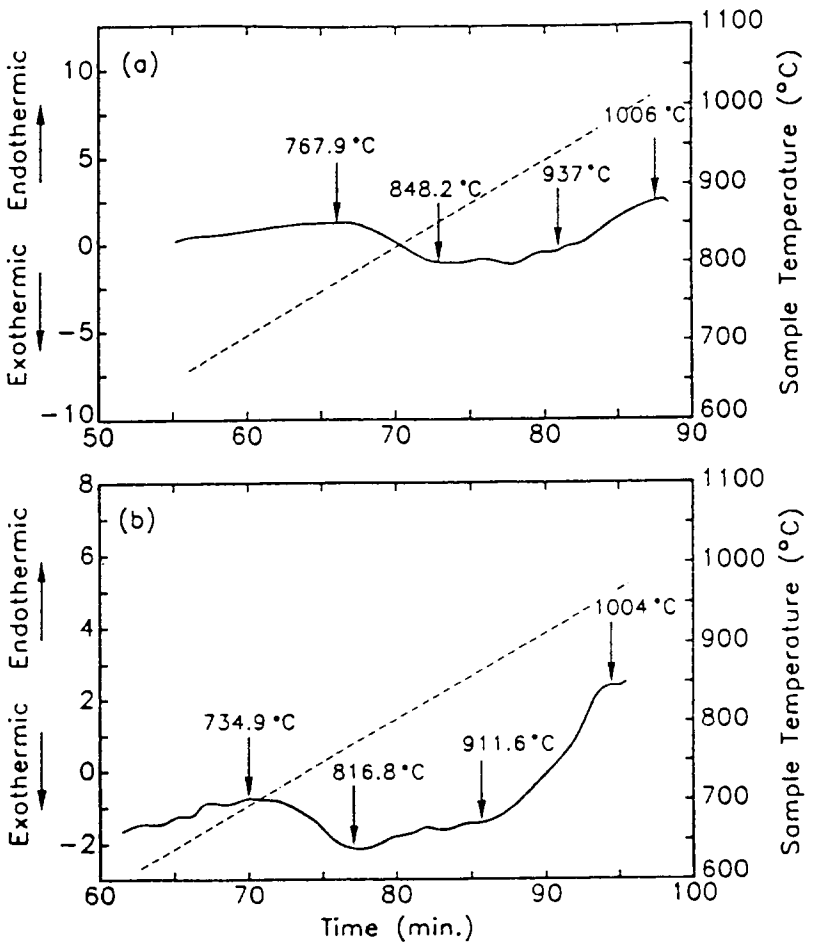

Fig. 2. (a) DTA curve for undoped B-4 base glass showing a glass crystallization temperature T_c of ~ 768°C. (b) DTA curve for as-quenched CdS-doped B-4 glass showing a crystallization temperature T_c of ~ 735°C.

CdS nuclei act as heterogeneous nucleation sites for bulk-crystal growth of the relevant oxide-crystalline phases in the glass matrix itself.

We also heat-treated a series of as-quenched CdS-doped glass samples in the range between T_g and T_c, producing high-quality samples revealing quantum confinement effects in the linear absorption spectra [20]. A summary of heat treatment temperatures in relation to the precipitation stages and achievement of a pronounced quantum confinement effect is shown in Fig. 3. The best heat-treatment range (between 577 and 735°C) for CdS quantum dots in B-4 silicate glass is explicitly identified in Fig. 3. Similar heat treatment maps can be obtained from DTA data for other quantum-dot/glass systems.

To compromise the low melting point and vaporization of CdTe, samples containing CdTe quantum dots [22, 31] were prepared by co-melting 2–3 wt% CdTe powder with another experimentally developed silicate glass, called B-9 base glass composition, as shown in Table 2. Most of the preparation procedures were the same as the above CdS or CdSe quantum dots except that the melting conditions were 1300°C for only one hour. To minimize the vaporization and maximize the solubility of the doped semiconductors, we adjusted the melting conditions (temperature and time) for doping different semiconductors in the glass matrices. However, the solubilities of CdS, CdSe, and CdTe in silicate glasses were low: from 1 to 3 wt% under the optimized melting conditions.

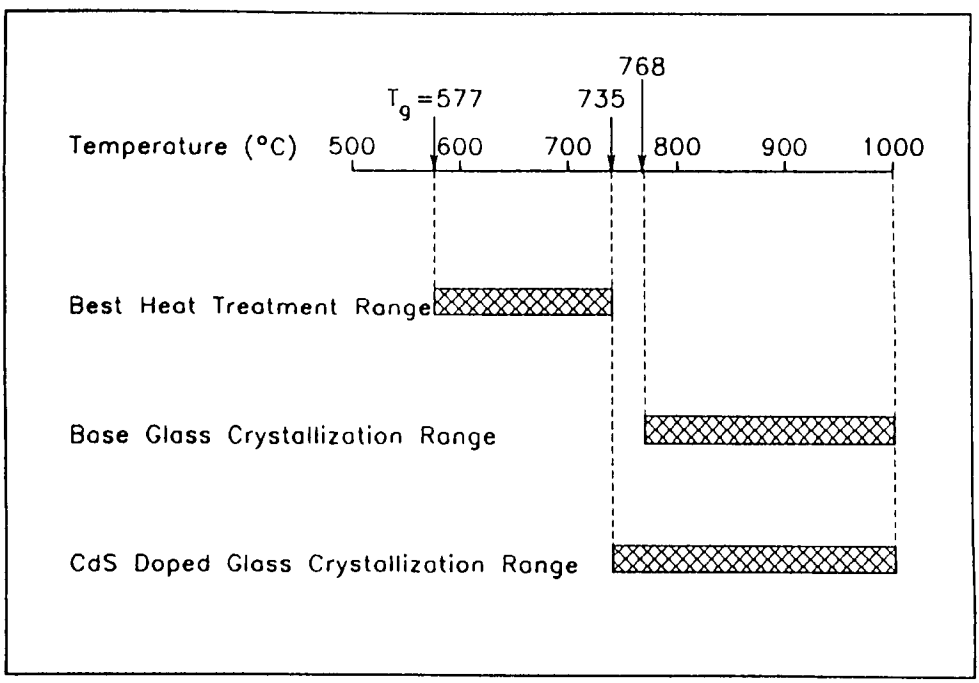

Fig. 3. Summary of heat treatment processing for CdS-doped B-4 glasses. The best heat treatment range yields CdSe quantum dots with strong quantum confinement. Temperature ranges corresponding to bulk glass crystallization (to oxide phases) are also shown for undoped and CdS-doped B-4 glasses.

Therefore, we tried to use other glass systems (phosphates) as the base glass composition for doping higher amounts of semiconductors.

4.2. CdSe quantum dots in phosphate glasses

Omi et al. [32] reported the capability of dissolving very high concentrations of CdSe (up to ~ 35 mol%) in phosphate glasses in the $CdO–P_2O_5$ and $ZnO–P_2O_5$ systems. We believed that precipitation of high-population-density quantum dots in these glasses might strongly enhance the third-order nonlinear optical susceptibility. Our attempts to duplicate the melts of compositions reported by Omi et al. showed that these glasses were unstable toward surface crystallization upon reheating to induce quantum-dot precipitation. DTA data in Fig. 4, which shows the glass crystallization starting from 574.9°C, exhibit this unstable feature of 50 $CdO–50P_2O_5$ (mol%) glass with added CdSe (18 mol%). Compared with CdS-doped B-4 glass, such a newly developed high-concentration CdSe-doped phosphate glass would have a much lower crystallization temperature [33].

In order to enhance the chemical stability of glasses, we therefore modified the phosphate glass batch by introducing CaO. We found that stable glasses with CdSe added up to ~ 14 mol% could be formed. The nominal base glass composition was (in mol%): 14 CaO–16 CdO–10 ZnO–60 P_2O_5. To produce this glass, we melted the glass batch containing CaO, CdO, ZnO, and $NH_4H_2PO_4$ powder at 1250°C for 2 h, then fast-quenched it to a clear, colorless base glass. The base glass powder mixed with 14 mol% CdSe was then melted at 1200°C for 20 min in a covered alumina crucible, then fast-quenched on a brass plate. Finally, the as-quenched CdSe-doped phosphate glasses were heat-treated at temperatures from 600 to 700°C for 20–60 min with no surface crystallization. The colors of the heat-treated CdSe-doped phosphate glasses changed from clear to dark brown, but not as bright red as the heat-treated CdSe-doped silicate glasses.

4.3. GaAs and Si quantum dots in silicate glasses

The newly developed porous silicon showing red luminescence inspired us to study the photoluminescence of silicon nanocrystals. We used the B-4 glass melt, dissolving and truncating the added silicon particles [25], instead of the HF-etched porous silicon technique. Silicon powder in pure form (NIST-standard reference materials 640b with average particle diameter < 10 μm) was blended with a pre-cast and ground powder of B-4 base glass. We added about 9 wt% of excess silicon powder to the glass powder and melted the batch at 1400°C for 6, 8, ..., and 18 h in an alumina crucible. This solidified to blackish-gray glassy masses containing unreacted silicon nanocrystals left behind due to incomplete dissolution or oxidation by the oxidic glass melt. The longer melting time made the glass lighter gray, or sometimes brownish gray, and finally it became as clear as the base glass after more than 10 h melting. Due to the continued reaction with the molten glass, it is reasonable to expect that the silicon remnants in the glass be reduced in size after each melting–casting sequence.

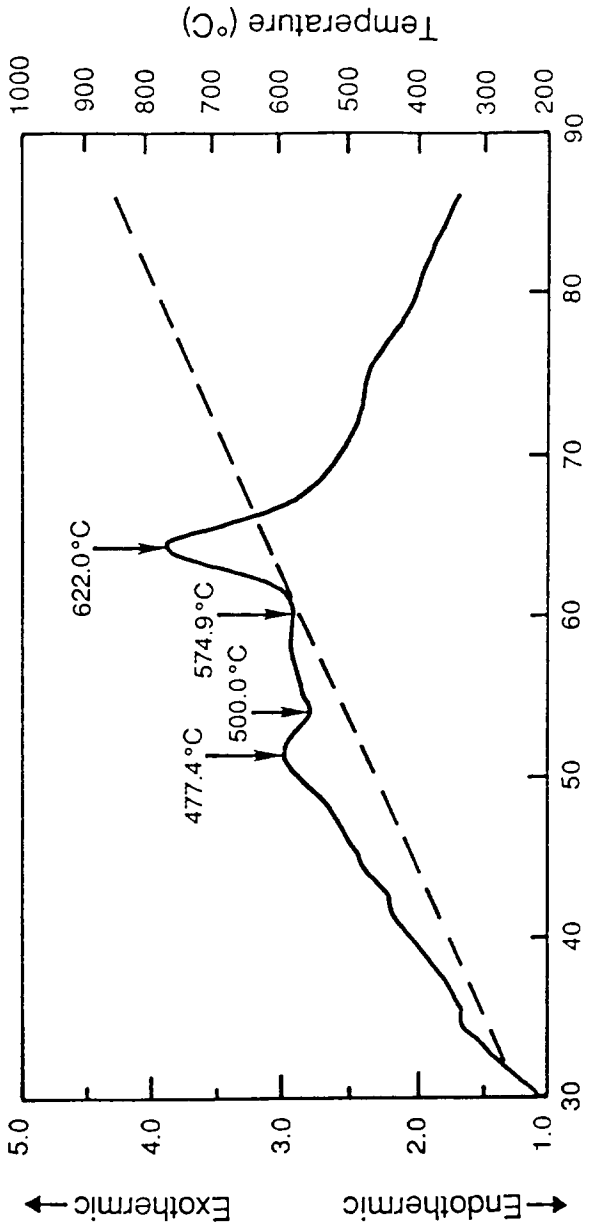

Fig. 4. DTA curve for 50 CdO 50 P_2O_5 (mol%) glass with added CdSe (18 mol%) showing a crystallization temperature T_c of ~ 575 C.

GaAs is a III-V compound semiconductor which cannot be precipitated from the silicate glass matrix after dissolving in the glass melt and fast-quenching. Therefore, we tried to make GaAs nanocrystals by dissolving GaAs and truncating them in the B-4 silicate glass [34,35]. This process differed from the above silicon-glass reaction process only in that the base glass and ~ 5 wt% GaAs mixture powder were melted at ~ 1300–1350°C for 25 min; such a melting condition compromised the decomposition and vaporization of Ga and As during the melting. The as-quenched glass contained unreacted GaAs particles, exhibiting an inhomogeneous blackish-gray color with a tiny region of brownish color.

5. Summary

Using the differential thermal analysis curves and linear absorption spectra as guides, the transformations and coalescence of CdS, CdSe, and CdTe quantum-dot glasses exhibiting quantum confinement effects were investigated. Although good samples for research can be obtained, the size distribution of dots in the glass is a persistent problem that needs further study. Special base glass compositions such as phosphate glasses are suitable for doping a high concentration of CdSe and other semiconductors. The thermodynamic stability of semiconductor-doped glasses and the doping concentration are two factors important in the application of these engineered structures. Nucleation and growth kinetics of these materials, modified LSW theory, and the connection of interface/surface states to optical properties continue to be fruitful areas of research.

Acknowledgements

I acknowledge the contributions of my former students Dr. Li-chi Liu and H. Brian Underwood. Support from NSF Grants DMR 90-06282 and DMR 94-11179, Electronic Materials Program is gratefully acknowledged.

References

[1] J. Bardeen and W.H. Brattain, Phys. Rev., 74 (1948) 230.
[2] C. Weisbuch and B. Vinter, Quantum Semiconductor Structures, Academic Press, Inc., San Diego, CA, 1991, p. 189.
[3] R. Rossetti and L.E. Brus, J. Phys. Chem. 86 (1982) 4470.
[4] L.E. Brus, J. Chem. Phys., 79 (1983) 5566.
[5] R. Rossetti, S. Nakahara and L.E. Brus, J. Chem. Phys., 79 (1983) 1086.
[6] R. Rossetti, J.L. Ellison, J.M. Gibson and L.E. Brus, J. Chem. Phys., 80 (1984) 4464.
[7] Y. Wang, A. Suna and W. Mahler, Mat. Res. Soc. Symp. Proc., 109 (1988) 197.
[8] A.I. Ekimov and A.A. Onushchenko, Pis'ma Zh. Eksp. Teor. Fiz., 40 (1984) 337.
[9] J. Warnock and D.D. Awschalom, Phys. Rev. B, 32 (1985) 5529.
[10] N.F. Borrelli, D.W. Hall, H.J. Holland and D.W. Smith, J. Appl. Phys., 61 (1987) 5399.

[11] B.G. Potter and J.H. Simmons, Phys. Rev. B, 37 (1988) 10838.
[12] V. Esch, A. Chavez-Pirson, L.C. Liu, S.H. Risbud, G. Khitrova, S.W. Koch and H.M. Gibbs, THNN5, Cong. on Laser and Electro-Optics (CLEO), Baltimore, MD, 1989.
[13] Y. Masumoto, M. Yamazaki and H. Sugawara, Appl. Phys. Lett., 53 (1988) 1527.
[14] Y. Wang and N. Herron, J. Phys. Chem., 91 (1987) 257.
[15] J.C. Luong and N.F. Borrelli, Mat. Res. Soc. Symp. Proc., 144 (1989) 695.
[16] M. Nogami, K. Nagaska and E. Kato, J. Am. Ceram. Soc., 73 (1990) 2097.
[17] M.A. Reed, J.N. Randall, R.J. Aggarwal, R.J. Matyi, T.M. Moore and A.E. Wetsel, Phys. Rev. Lett., 60 (1988) 535.
[18] J.N. Randall, M.A. Reed, T.M. Moore, R.J. Matyi and J.W. Lee, J. Vac. Sci. Technol. B, 6 (1988) 302.
[19] K. Tsunetomo, H. Nasu, H. Kitayama, A. Kawabuchi, Y. Osaka and K. Takiyama, Jpn. J. Appl. Phys., 28 (1989) 1928.
[20] L.C. Liu and S.H. Risbud, J. Appl. Phys., 68 (1990) 28.
[21] F. Hache, D. Ricard and C. Flytzanis, Appl. Phys. Lett., 55 (1989) 1504.
[22] V. Esch, B. Fluegel, G. Khitrova, H.M. Gibbs, X. Jiajin, K. Kang, S.W. Koch, L.C. Liu, S.H. Risbud and N. Peyghambarian, Phys. Rev. B, 42 (1990) 7450.
[23] L.T. Canham, Appl. Phys. Lett., 57 (1990) 1046.
[24] Y.H. Xie, W.L. Wilson, F.M. Ross, J.A. Mucha, E.A. Fitzgerald, J.M. Macaulay and T.D. Harris, J. Appl. Phys., 71 (1992) 2403.
[25] S.H. Risbud, L.C. Liu and J.F. Shackelford, Appl. Phys. Lett., 63 (1993) 1648.
[26] L.C. Liu and S.H. Risbud, J. Appl. Phys., 76 (1994) 4576.
[27] J. Zarzycki, Glasses and the Vitreous State, Cambridge University Press, Cambridge, 1991, p. 288.
[28] Y. Fuyu and J.M. Parker, Mater. Lett., 6 (1988) 233.
[29] Y. Fuyu, J.M. Parker and B.J. Ainslie, J. Phys. D: Appl. Phys., 21 (1988) S82.
[30] A.I. Ekimov, A.L. Efros and A.A. Onushchenko, Solid State Commun., 56 (1985) 921.
[31] L.C. Liu, M.J. Kim, S.H. Risbud and R.W. Carpenter, Philos. Mag. B, 63 (1991) 769.
[32] S. Omi, H. Hiraga, K. Uchida, C. Hata, Y. Asahara, A.J. Ikushima, T. Tokizaki and A. Nakamura, 11th Congress on Lasers and Electro-Optics (CLEO'91), Baltimore, MD, 1991.
[33] L.C. Liu, H.B. Underwood and S.H. Risbud, in L.D. Pye, W.C. LaCourse and H.J. Stevens (Eds.), The Physics of Non-Crystalline Solids, Soc. Glass. Technol., Taylor and Francis, London, 1992, p. 523.
[34] L.C. Liu and S.H. Risbud, in P.D. Persans, J.S. Bradley, R.R. Chianelli and G. Schmid (Eds.), Chemical Processes in Inorganic Materials: Metals and Semiconductor Clusters and Colloids, Mat. Res. Soc. Symp. Proc., Vol. 272, San Francisco, CA, 1992, p. 35.
[35] S.H. Risbud and H.B. Underwood, J. Mater. Syn. Proc., 1 (1993) 225.